



HAL
open science

Oxygen Ions O^+ Energized by Kinetic Alfvén Eigenmode During Dipolarizations of Intense Substorms

Suping Duan, Lei Dai, Chi Wang, Zhaohai He, Chunlin Cai, Y. C. Zhang, I. Dandouras, H. Reme, M. André, Y. V. Khotyaintsev

► **To cite this version:**

Suping Duan, Lei Dai, Chi Wang, Zhaohai He, Chunlin Cai, et al.. Oxygen Ions O^+ Energized by Kinetic Alfvén Eigenmode During Dipolarizations of Intense Substorms. *Journal of Geophysical Research Space Physics*, 2017, 122, pp.11,256-11,273. 10.1002/2017JA024418 . insu-03676809

HAL Id: insu-03676809

<https://insu.hal.science/insu-03676809>

Submitted on 24 May 2022

HAL is a multi-disciplinary open access archive for the deposit and dissemination of scientific research documents, whether they are published or not. The documents may come from teaching and research institutions in France or abroad, or from public or private research centers.

L'archive ouverte pluridisciplinaire **HAL**, est destinée au dépôt et à la diffusion de documents scientifiques de niveau recherche, publiés ou non, émanant des établissements d'enseignement et de recherche français ou étrangers, des laboratoires publics ou privés.

Copyright

RESEARCH ARTICLE

10.1002/2017JA024418

Key Points:

- Energetic O^+ ion (>1 keV) flux increases significantly during intense substorm ($AE > 500$ nT) dipolarizations
- O^+ ions are energized by KAWE mostly in the direction perpendicular to the magnetic field in the PSBL
- KAWE can play an important role in the process of O^+ ions transferred from the lobe/PSBL into the plasma sheet during intense substorms

Correspondence to:

S. Duan,
spduan@nssc.ac.cn

Citation:

Duan, S., Dai, L., Wang, C., He, Z., Cai, C., Zhang, Y. C., ... Khotyaintsev, Y. V. (2017). Oxygen ions O^+ energized by kinetic Alfvén eigenmode during dipolarizations of intense substorms. *Journal of Geophysical Research: Space Physics*, 122, 11,256–11,273. <https://doi.org/10.1002/2017JA024418>

Received 31 MAY 2017

Accepted 24 OCT 2017

Accepted article online 31 OCT 2017

Published online 14 NOV 2017

Oxygen Ions O^+ Energized by Kinetic Alfvén Eigenmode During Dipolarizations of Intense Substorms

Suping Duan¹ , Lei Dai¹ , Chi Wang¹ , Zhaohai He¹, Chunlin Cai¹, Y. C. Zhang¹, I. Dandouras^{2,3}, H. Reme^{2,3} , M. André⁴ , and Y. V. Khotyaintsev⁴ 

¹State Key Laboratory of Space Weather, National Space Science Center, Chinese Academy of Sciences, Beijing, China, ²University of Toulouse, UPS-OMP, IRAP, Toulouse, France, ³CNRS, IRAP, Toulouse, France, ⁴Swedish Institute of Space Physics, Uppsala, Sweden

Abstract Singly charged oxygen ions, O^+ , energized by kinetic Alfvén wave eigenmode (KAWE) in the plasma sheet boundary layer during dipolarizations of two intense substorms, 10:07 UT on 31 August 2004 and 18:24 UT on 14 September 2004, are investigated by Cluster spacecraft in the magnetotail. It is found that after the beginning of the expansion phase of substorms, O^+ ions are clearly energized in the direction perpendicular to the magnetic field with energy larger than 1 keV in the near-Earth plasma sheet during magnetic dipolarizations. The pitch angle distribution of these energetic O^+ ions is significantly different from that of O^+ ions with energy less than 1 keV before substorm onset that is in the quasi-parallel direction along the magnetic field. The KAWE with the large perpendicular unipolar electric field, $E_z \sim -20$ mV/m, significantly accelerates O^+ ions in the direction perpendicular to the background magnetic field. We present good evidences that O^+ ion origin from the ionosphere along the magnetic field line in the northward lobe can be accelerated in the perpendicular direction during substorm dipolarizations. The change of the move direction of O^+ ions is useful for O^+ transferring from the lobe into the central plasma sheet in the magnetotail. Thus, KAWE can play an important role in O^+ ion transfer process from the lobe into the plasma sheet during intense substorms.

1. Introduction

O^+ ions solely originating from the ionosphere play a key role in the energy and mass transfer during substorms (e.g., Daglis et al., 1994; Duan et al., 2015; Keika et al., 2013; Kronberg et al., 2014; Liao et al., 2015; Moukikis et al., 2010; Nilsson et al., 2016; Ohtani et al., 2011; Sauvaud et al., 2012; Seki et al., 2001; Welling et al., 2015). Daglis et al. (1994) reported that the energy density of O^+ ions in the near-Earth magnetotail was correlated with substorm activity. Daglis and Axford (1996) suggested that the nightside auroral outflow could provide a fast feeding of energetic O^+ ions in the near-Earth magnetotail during substorms. Baker et al. (1985) reported that the ionospheric oxygen ions could play an important role in the location and initiation of plasma sheet instabilities during substorms.

It is well known that the ionosphere is the exclusive source of O^+ ions. The dayside cusp and the nightside auroral region are the main sources of O^+ outflow (e.g., Liao et al., 2010; Yau & André, 1997; Yu & Ridley, 2013). The geomagnetic activity has significant effect on the outflow of O^+ ions from the ionosphere (e.g., Peromian et al., 2006; Yau et al., 1985). Lennartsson and Shelley (1986) found that the O^+/H^+ ratio increases in positive relationship with high AE index around local midnight ($AE \sim 1,000$ nT). Maggolo and Kistler (2014) reported that the geomagnetic activity had larger effect on O^+ density than solar EUV flux in the Earth midtail ($\sim 15\text{--}20 R_E$). The O^+ density increases significantly by a factor of ~ 10 during low geomagnetic activity and by a factor of ~ 31 during high activity. While solar EUV flux has small effect on the O^+ density. The O^+ density increases by a factor of ~ 3.5 during high solar activity.

O^+ ions play a key role in the substorm processes, especially, in the expansion phase of substorms. Baker et al. (1982) suggested that the enhancement of O^+ ions in the plasma sheet would trigger substorm onset as O^+ ions caused tearing mode instabilities. Daglis et al. (1994) pointed out that O^+ energy density had a strong correlation with the preonset electrojet activity, that is, AU index, in the near-Earth plasma sheet (NEPS). It means that the ionospheric precipitation may be an effect of the driven component of substorms. And this correlation implies that the acceleration of O^+ ions from the ionosphere is at late growth phase of substorms. There is a good correlation between the energy density of O^+ ions and AE index (Daglis et al., 1994).

Especially, O^+ energy density explosively increases during the intense substorm expansion phase with AE index larger than 500 nT (Daglis et al., 1994). Lennartsson and Shelley (1986) reported that O^+ ion number density sharply increases with the AE index larger than 500 nT. Daglis and Axford (1996) found that the rapid enhancement of O^+ ion energy fluxes occurred in the inner magnetotail after substorm onset. Winglee and Harnett (2011) suggested that O^+ ions provide almost 50% of the total energy density in NEPS just before onset time.

O^+ ion outflow from the ionosphere with very low energy $\sim eV$ is transferred into the NEPS in the magnetotail and energized to approximately tens of keV (e.g., Kistler, 2017; Yau et al., 1985, 2012). Geotail observations present an evidence of ion mass-dependent energization in the range of 10 KeV/e to 210 KeV/e during substorms in the NEPS (e.g., Kistler et al., 1990; Nosé et al., 2000). Kronberg et al. (2014) reported that the mass selective ion energization was possibly caused by the induced electric field as a result of the time variation of the magnetic field during substorm dipolarization. Delcourt et al. (1990) pointed out that O^+ ions with gyroperiods comparable to the dipolarization timescale are energized by the induced electric field during this nonadiabatic process. But proton with smaller gyroperiod may be transported adiabatically. Fok et al. (2006) reported that O^+ ion energy prompt enhancement during dipolarization was a result of nonadiabatic heating of the low-energy O^+ ions stored in the plasma sheet before substorms. Lindstedt et al. (2010) shown that O^+ ions are energized by intense localized electric field at the boundary between the lobe and the high-altitude cusp.

The acceleration of O^+ ions by low-frequency waves was observed in the PSBL (e.g., Grigorenko, Burinskaya, et al., 2010; Grigorenko, Koleva et al., 2010; Grigorenko et al., 2011; Hirahara et al., 1994; Takada, Seki, Hirahara, Fujimoto, et al., 2005; Takada, Seki, Hirahara, Terasawa, et al., 2005). The ions perpendicular acceleration was caused by the $\mathbf{E} \times \mathbf{B}$ drift. This results in ions move from the lobe to the plasma sheet. The strong E_y component and B_x component is useful for this drift mechanism. But the electric field is variable in the PSBL, especially, the E_z component is the dominant (Duan et al., 2016).

Kinetic Alfvén waves with strong electric fields (e.g., Chen et al., 2015; Chen et al., 2013; Klimushkin & Mager, 2014; Lee et al., 1994; Liang et al., 2016; Lin et al., 2012; Wu & Chen, 2013) are observed in the near-Earth plasma sheet, especially in the plasma sheet boundary layer in the magnetotail during substorms (e.g., Duan et al., 2016; Keiling, 2009; Wygant et al., 2005). Duan et al. (2016) reported that kinetic Alfvén wave eigenmode (i.e., KAW) with unipolar pulse electric field, $E_z \sim -30$ mV/m, was firstly observed in the plasma sheet boundary layer during magnetic dipolarizations. The generation of KAW corresponds to the Hall effect in the magnetic reconnection (Dai, 2009; Dai, Wang, Angelopoulos, 2015; Dai et al., 2017). KAW consists of strong out-of-plane magnetic field and electric field normal to the PSBL. This intense unipolar pulse electric field of KAW has potential to interact with ions from the lobe. Kronberg et al. (2014) also proposed that some acceleration of O^+ ions was at work in the direction perpendicular to the magnetic field in the boundary layer with a strong electric field ~ 20 mV/m.

The transport pathway and energization mechanism of O^+ ions from the ionosphere to the NEPS are interesting subject that still remains to be understood. The purpose of this investigation is to provide evidence of a new acceleration mechanism that transfers O^+ ions from the lobe into the plasma sheet during intense substorm dipolarization process. In section 2, we present two intense substorm events that provide detailed observations of O^+ ion energy flux and KAW eigenmode structure in the tail plasma sheet during the substorm expansion phase. Then we describe the close relationship between KAW eigenmode and O^+ ion energization during intense substorm dipolarizations. Summary is presented in section 3.

2. Data Analysis

In this study we use Cluster data from the Cluster ion spectrometry/Composition and Distribution Function (CIS/CODIF) (Rème et al., 2001), Fluxgate Magnetometer (FGM) (Balogh et al., 2001), and Electric Field and Wave (EFW) (Gustafsson et al., 2001) instruments that obtained from Cluster Active Archive (Laakso et al., 2010) to investigate the acceleration of O^+ ions during two intense substorm dipolarizations. The Cluster spacecraft was located in the midmagnetotail around $X \sim -16 R_E$. The CIS/CODIF instrument measures the 3-D distributions of major ions, such as H^+ , He^+ , and O^+ within the energy range from 40 eV/e to 40 keV/e with temporal resolutions of 4–16 s (Rème et al., 2001). Cluster spacecraft provides a good chance to

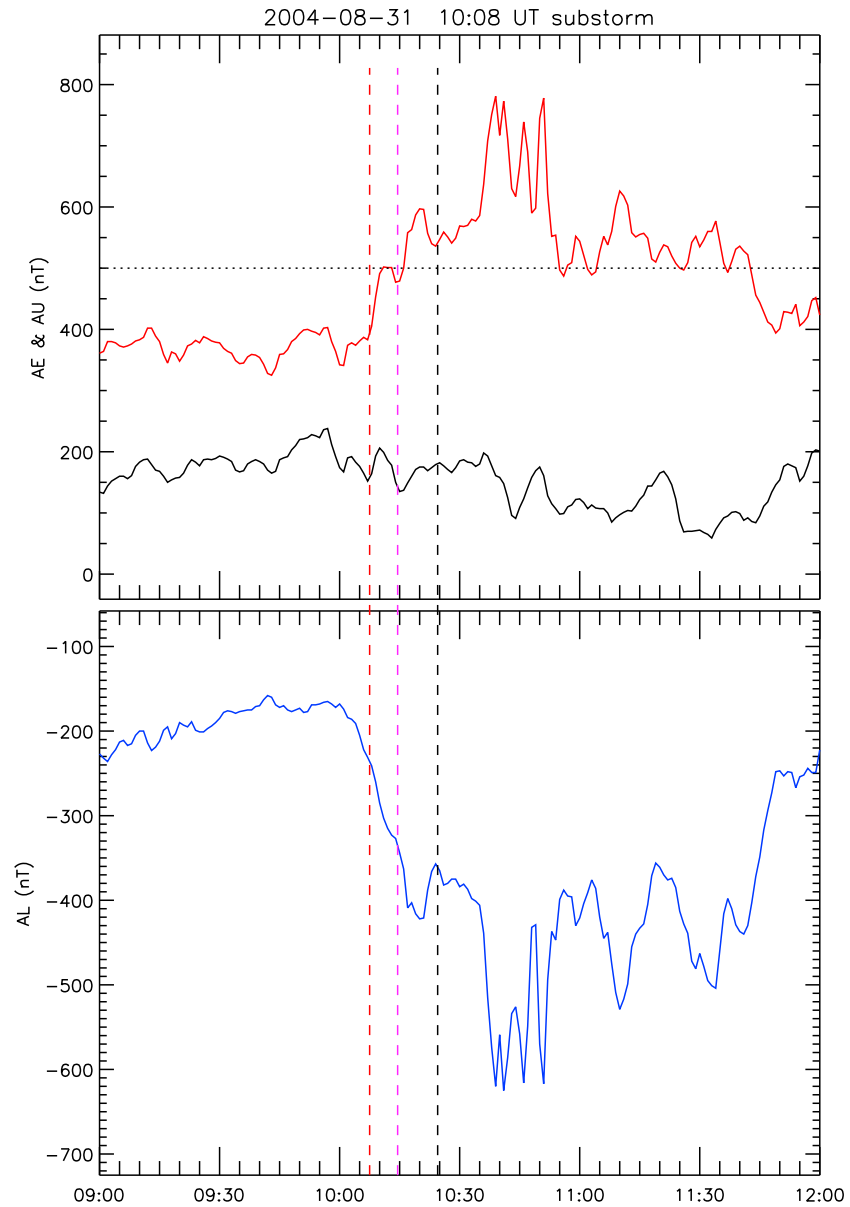


Figure 1. The *AU*, *AL*, and *AE* index on 31 August 2004. The first vertical dashed red line marks the substorm onset time. The second and third vertical dashed lines mark two beginning time of this substorm enhancements.

detect O^+ ion energization during its tail seasons. Two intense substorms on 31 August 2004 and 14 September 2004 are presented in this investigation.

2.1. Event of 31 August 2004

Figure 1 presents the *AU* (black line), *AL* (blue line), and *AE* (red line) indices during the period from 09:00 UT to 12:00 UT on 31 August 2004. The *AL* index decreases sharply at 10:00 UT, and the *AE* index increases gradually from 350 nT at 10:07 UT and then *AE* index has multiple step increase. Thus, the substorm onset time is identified at around 10:07 UT, as marked by the vertical red line in Figure 1. The *AU* index is high before substorm onset. *AU* index maximum value is about 250 nT. *AE* index begins to be larger than 500 nT at 10:15 UT. The maximum value of *AE* index during the time intervals we focus on is about 750 nT. It implies that this substorm is an intense one.

During this intense substorm expansion phase Cluster C1 was located at around $(-15.1, -1.1, 4.8) R_E$ and C4 located at around $(-15.2, -1.2, 4.7) R_E$ in the Earth magnetotail. These two spacecraft are located very closed

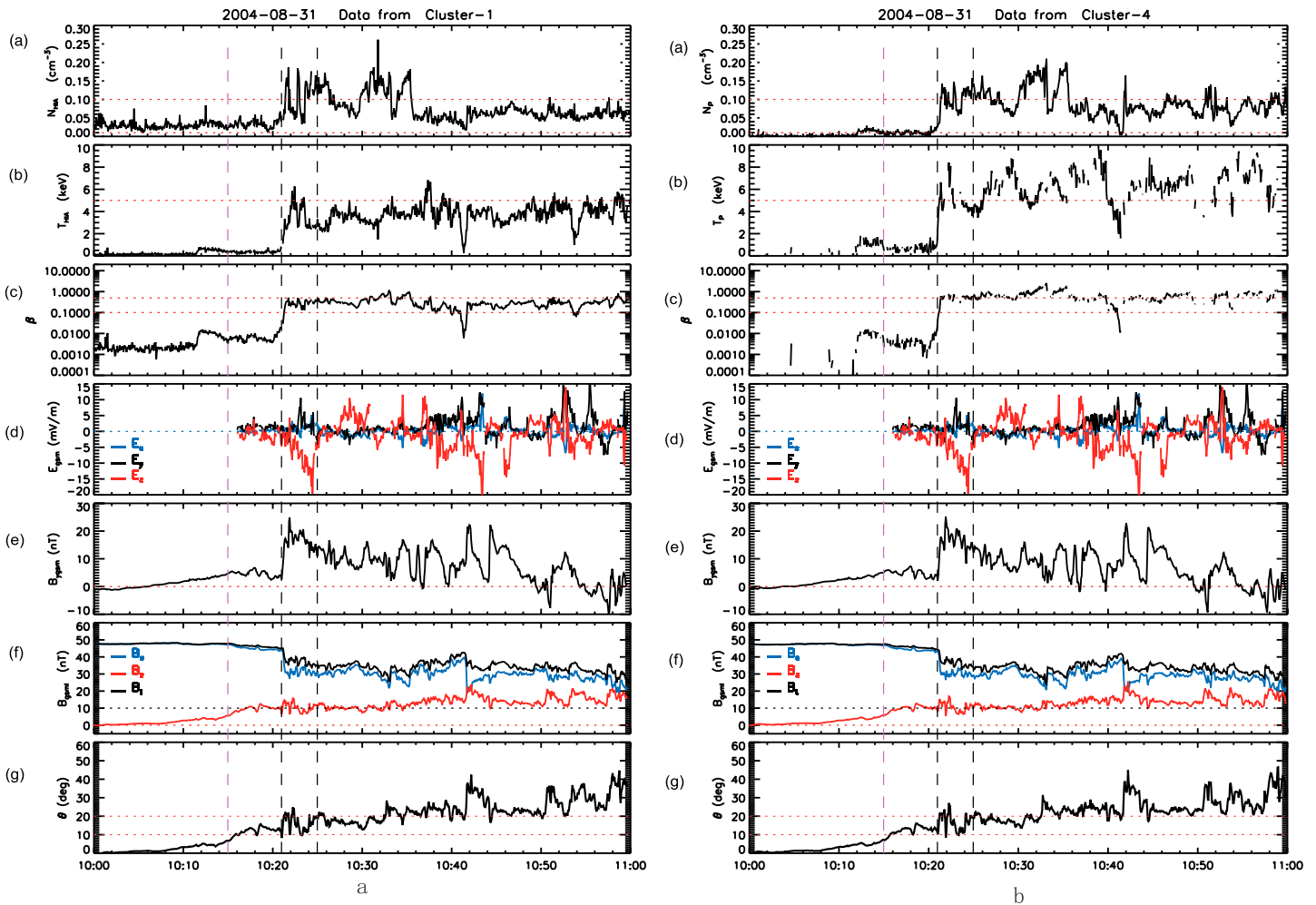


Figure 2. (Figure 2a) The plasma and electromagnetic field detected by Cluster C1 in the interval of 10:00 UT to 11:00 UT on 31 August 2004 in the magnetotail. (a) Ion number density; (b) ion temperature; (c) plasma beta value, β ; (d) the three components of the electric field E_x (blue), E_y (black), and E_z (red); (e) the B_y component of the magnetic field, B_y ; (f) the B_x (blue) and B_z (red) components and the total magnitude of magnetic field, B_t (black); and (g) the magnetic field elevation angle, θ . The first vertical dashed red line marks the substorm first enhancement time. The second and third vertical dashed lines mark unipolar electric field interval time of this substorm. (Figure 2b) The plasma and electromagnetic field detected by Cluster C4 in the interval of 10:00 UT to 11:00 UT on 31 August 2004 in the magnetotail. (a) Proton number density; (b) proton temperature; (c) plasma beta value, β ; (d) the three components of the electric field E_x (blue), E_y (black), and E_z (red); (e) the B_y component of the magnetic field, B_y ; (f) the B_x (blue) and B_z (red) components and the total magnitude of magnetic field, B_t (black); and (g) the magnetic field elevation angle, θ .

to each other with distance about 1,000 km. The plasma and electromagnetic field parameters from the CIS/CODIF, FGM, and EFW instruments on Cluster spacecraft all indicate that Cluster SC crossed through the lobe, plasma sheet boundary layer (PSBL), and into plasma sheet from 10:00 UT to 11:00 UT, which is presented in Figure 2. The GSM coordinate systems are adopted.

The plasma and electromagnetic field data observed by Cluster C1 and C4 from 10:00 UT to 11:00 UT on 31 August 2004 are presented in Figures 2a and 2b, respectively. From top to bottom, the plots present ion (proton) number density, N_{ion} (N_p); ion (proton) temperature, T_{ion} (T_p); plasma beta value, β ; the electric field E_x (blue), E_y (black), and E_z (red) components; the B_y component; the B_x (blue), B_z (red) and total magnitude of magnetic field, B_t (black); and the magnetic field elevation angle, θ . EFW measures electric field in the spacecraft spin plane, and the third (not measured) component of E is computed using condition of zero parallel electric field, $\mathbf{E} \cdot \mathbf{B} = 0$ (scalar product) (Dai et al., 2013; Khotyaintsev et al., 2010). This method is good in our event for the larger angle between the magnetic field and the spin plane. The first substorm enhancement beginning time, $\sim 10:15$ UT, is marked by the vertical dotted purple line. The interval period between two vertical dotted black lines is with the intense E_z and B_y disturbance and magnetic dipolarization. During

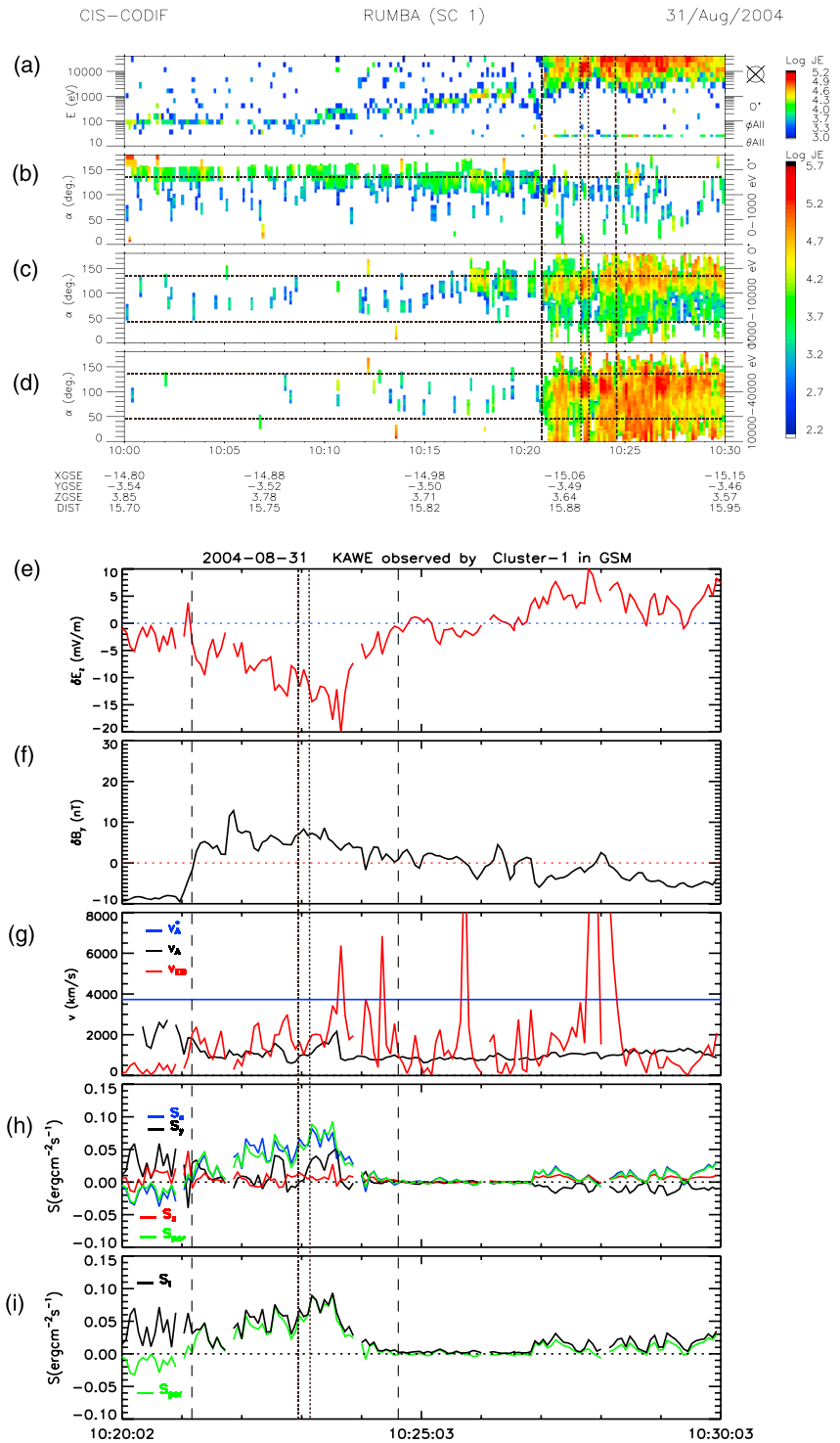


Figure 3. The O^+ ion energy spectrogram flux obtained from CODIF (energy range is from 40 eV to 40 keV) and unipolar electromagnetic field fluctuations observed by Cluster C1 during intense substorm on 31 August 2004. (a) O^+ energy spectrogram of omnidirectional flux. (b–d) O^+ pitch angle distribution with energy in the range of 40 eV to 1 keV, 1 keV to 10 keV, and 10 keV to 40 keV, respectively. (e) The perturbations of the z component of the electric field; (f) the perturbations of the y component of the magnetic field; (g) local Alfvén speed, V_A (black), predicted propagation speed of KAW eigenmode, V_A^* (blue), and the ratio of the perturbation electric (δE_z) to magnetic (δB_y) fields, $V_{\delta EB}$ (red); (h) three components of Poynting flux— S_x (blue), S_y (black), and S_z (red)—and the parallel Poynting flux along the magnetic field, S_{para} (green). (i) The total and parallel Poynting flux: S_T (black) and S_{para} (green). Two vertical dashed lines mark unipolar electric field interval time of this substorm.

this period the maximum value of the electromagnetic fluctuation of the $-E_z$ and B_y is 20 mV/m and 15 nT, respectively, as presented in Figures 2ad and 2bd, and 2ae and 2be.

At $\sim 10:21$ UT, the second substorm enhancement beginning time, a fast magnetic dipolarization was observed by Cluster C1 and C4, marked by two vertical dashed black lines in Figures 2a and 2b. Around 10:21 UT, Cluster C1 and C4 were both in the PSBL, as indicated by the B_x (35 nT) and plasma beta (0.4). The dipolarization can be clearly identified as the increase in the B_z and the elevation angle. In the NEPS, the magnetic dipolarization is an indicator for a sudden collapse of the magnetotail (Baumjohann et al., 1999; Dai et al., 2014; Dai, Wang, Duan, et al., 2015; Duan et al., 2011; Lui et al., 1999; Nagai, 1982; Nakamura et al., 2009). Cluster C1 and C4 both observed a second dipolarization around 10:21 UT (the first dipolarization around 10:15 UT). The plasma sheet began to expand after 10:21 UT. The β increased to ~ 0.5 from 0.1. It means that Cluster C1 and C4 go through PSBL resulting from this dipolarization. During the second dipolarization, the significant electromagnetic pulses are observed. The pulses contain an intense negative E_z component and positive B_y component. The intervals of pulses, from 10:21 UT to 10:25 UT, are highlighted by two vertical dashed black lines.

2.2. Observations of O^+ Ions Energized by KAWE During Dipolarization

During this intense substorm, the energy flux of O^+ ions from Cluster C1 during the period of 10:00 UT to 10:30 UT on 31 August 2004 is presented in Figure 3a. Figures 3b–3d show the pitch angle distribution of O^+ ions with energy range from 40 eV to 1 keV, 1 keV to 10 keV, and 10 keV to 40 keV, respectively. The low-energy O^+ ion distribution changed from the quasi-parallel to quasi-perpendicular direction at the first magnetic dipolarization time around 10:15 UT as shown in Figure 3b. In the interval time of 10:21 UT to 10:25 UT, energy flux of O^+ ions with 1–40 keV increased significantly and these O^+ ions were mainly perpendicular pitch angle distribution, as presented in Figure 3c. As shown in Figures 2c and 2f, the plasma beta is less than 0.5 and the x component of the magnetic field is around 30 nT, approaching the total magnetic field value. These two parameters indicate that Cluster is located at the plasma sheet boundary layer during the period of 10:21 UT to 10:25 UT. Within these intervals the intensive unipolar electromagnetic fluctuation with negative E_z and positive B_y is observed, which is presented in Figures 3e and 3f, respectively.

Figure 3e presents that the magnitude of electric field pulses δE_z was -20 mV/m. The homologous magnetic field δB_y fluctuations are about 8 nT, as shown in Figure 3f. Figure 3g shows that the observed ratio $\delta E_z/\delta B_y$ is in the range from 1,000 km/s to 7,000 km/s, larger than v_A (the local Alfvén speed) during this intense negative E_z intervals. The Poynting flux, as shown in Figures 3h and 3i, is mostly along the magnetic field toward Earth, $0.08 \text{ erg cm}^{-2} \text{ s}^{-1}$. The $\delta E_z/\delta B_y$ ratio and unipolar electromagnetic pulses both provide strong evidences that these intense unipolar perturbations are KAWE (Duan et al., 2016).

During this intense substorm dipolarization, the similar observation results from Cluster C4 are presented in Figure 4. Because of the distance from Cluster C4 to the plasma sheet is smaller than the distance from Cluster C1, Cluster C4 first detected the PSBL at around 10:21 UT.

The unipolar pulse electric field of KAWE was both observed by C1 and C4 in the period of 10:21:00 UT to 10:24:40 UT in the PSBL, as shown in Figures 3e and 4e. During this period energetic O^+ ions were energized in the direction perpendicular to the background magnetic field, as presented in Figures 3c and 3d and Figures 4c and 4d. Figures 5a and 5b show two examples of 2-D cuts (the v_x - v_y plane and v_x - v_z plane) through the 3-D distributions of O^+ ion velocity observed by C4 at 10:22:52 UT and 10:23:08 UT, which are marked by the two vertical dotted lines in Figure 4, respectively. Similarly, Figures 5c and 5d present the O^+ ion velocity distributions by C1 at 10:22:54 UT and 10:23:11 UT, which are marked by the two vertical dotted lines in Figure 3, respectively. These cuts indicate that energetic O^+ ions (>1 keV) mainly flow in the southward direction with negative value of the v_z component. It is coincident of the pitch angle distribution of O^+ ions in the direction perpendicular to the magnetic field, as marked by the two vertical dotted lines in Figures 3 and 4. The increase in magnitude of $-v_z$ is from 200 km/s to 700 km/s. Then O^+ ions can be transferred from PSBL into the plasma sheet.

The intense unipolar electromagnetic pulses observed by Cluster C1 and C4 are identified as KAWE, as shown in Figures 3e–3g and 4e–4g. During the intense KAWE period, O^+ ions were accelerated in the

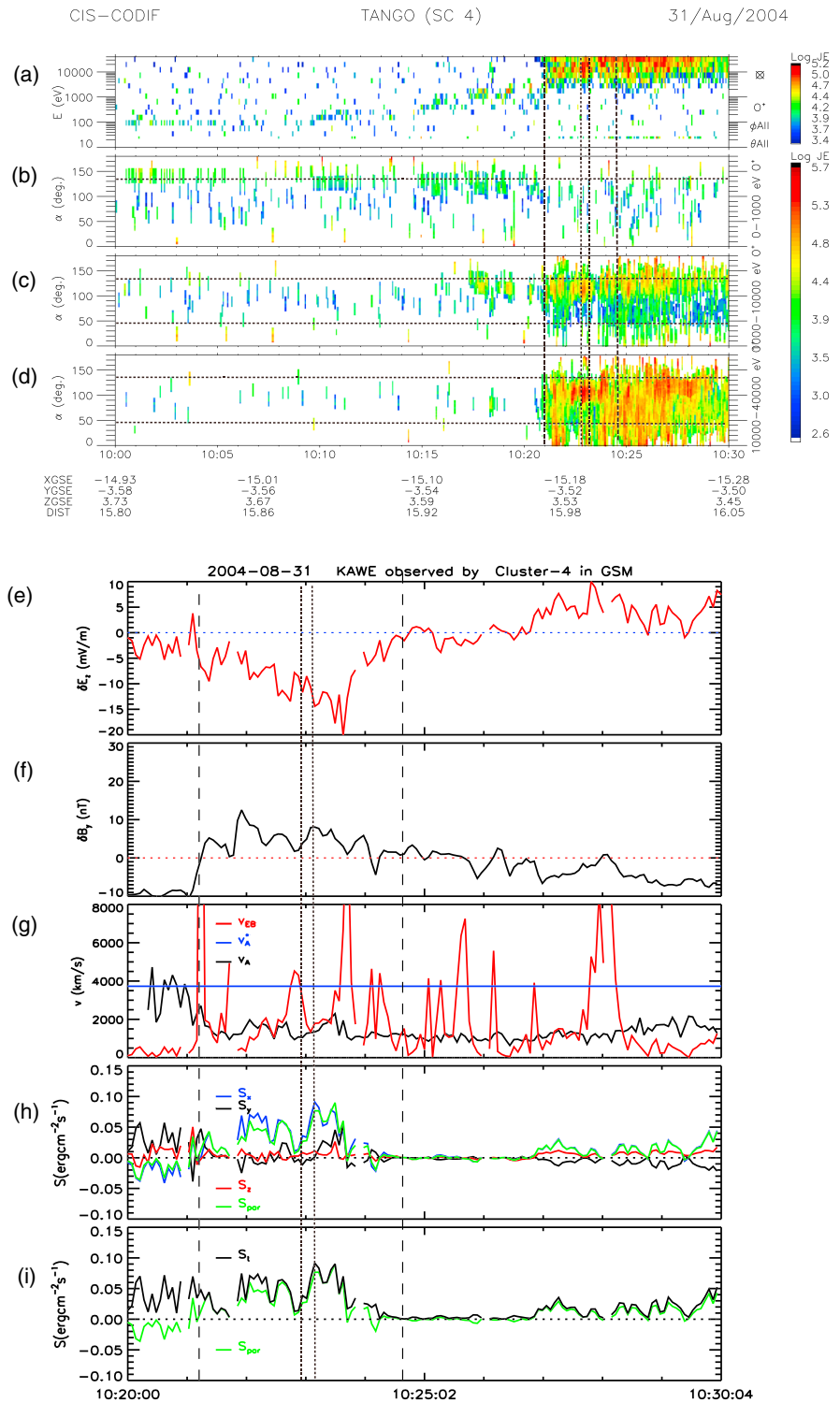


Figure 4. The O^+ ion energy spectrogram flux obtained from CODIF and unipolar electromagnetic field fluctuations observed by Cluster C4 during intense substorm on 31 August 2004. The figure formation is the same as Figure 3.

direction perpendicular to the background magnetic field, as shown with perpendicular pitch angle distribution of energetic O^+ ions (>1 keV) in Figures 3c and 4c, and the magnitude of southward V_z component enhancement in Figure 5. As a result, O^+ ions can pass through the PSBL into the central plasma sheet.

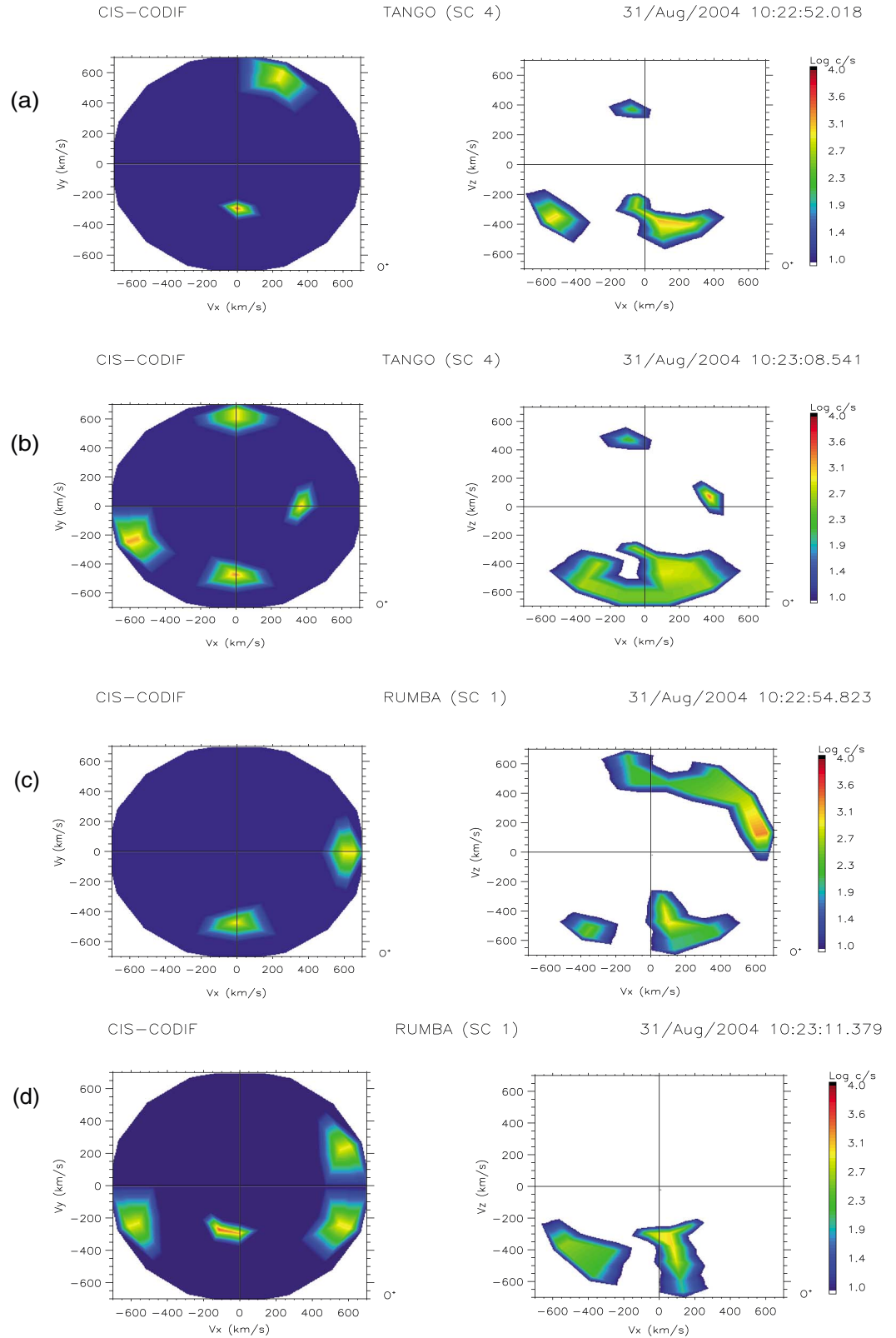


Figure 5. Two-dimensional cuts of the three-dimensional O^+ ion velocity distributions obtained by CODIF/C1 at 10:22:54 UT and 10:23:11 UT, respectively, and by CODIF/C4 at 10:22:52 UT and 10:23:08 UT, respectively, as marked by the two vertical dotted lines in Figures 3 and 4, respectively.

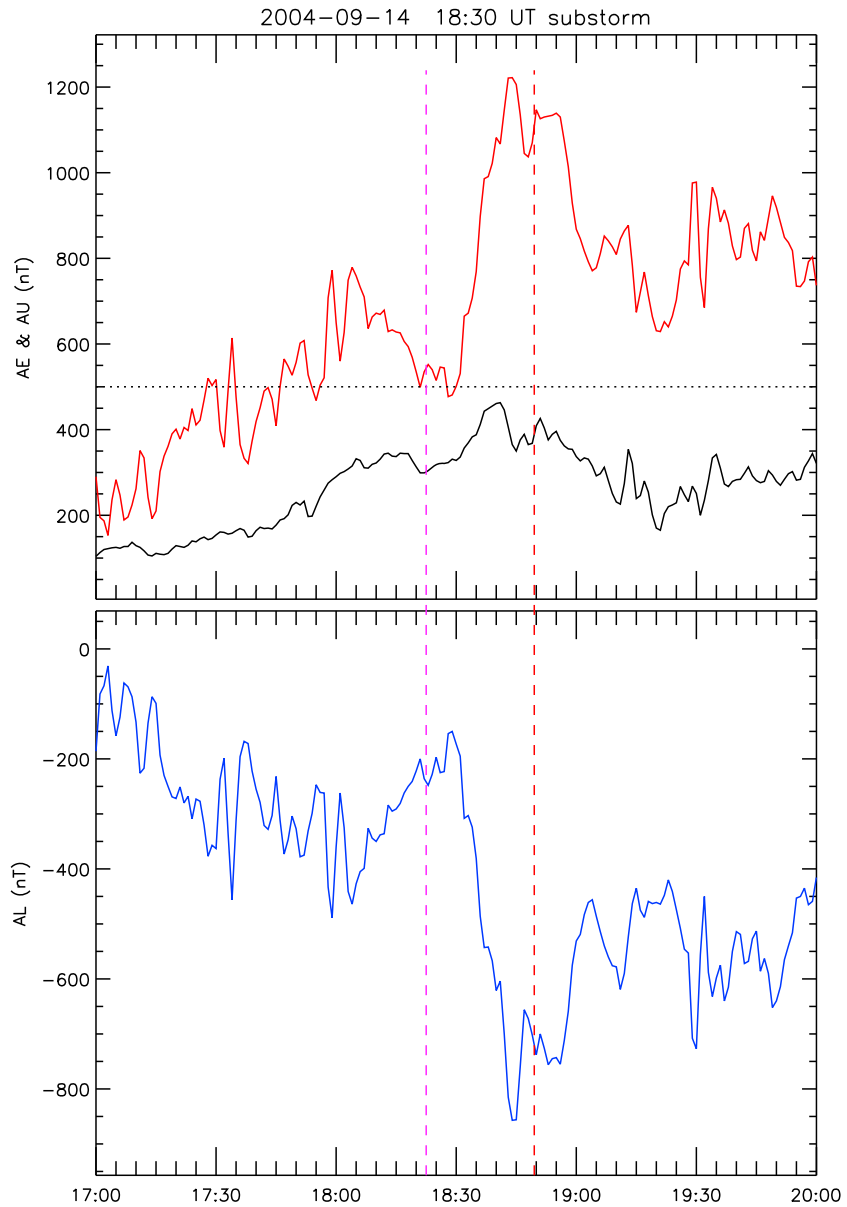


Figure 6. AE/AU/AL index in the interval of 17:00 UT to 20:00 UT on 14 September 2004. The purple vertical dashed line marks the substorm onset time of expansion phase, 18:24 UT. The vertical dashed red line marks a substorm enhancement at 18:50 UT.

2.3. Another Similar Event of 14 September 2004

Another similar event of O^+ ions energized by KAWE is observed by Cluster spacecraft on 14 September 2004. Figure 6 presents the AU, AL, and AE index of this event. The maximum value of AE index is around 1,200 nT. The first vertical purple line marks the onset time of intense substorm expansion phase, 18:24 UT. On the other hand, according to the auroral images from Imager for Magnetopause-to-Aurora Global Exploration spacecraft, the onset time is 18:24:41 UT (Frey et al., 2004). The vertical dashed red line marks a substorm enhancement at ~18:50 UT.

During this intense substorm expansion phase Cluster C1 is located at around $(-16.4, 1.6, 2.1) R_E$ and C4 is located at around $(-16.5, 1.5, 2.1) R_E$ in the magnetotail. These two spacecraft are located very close each other with distance about 1,000 km. The plasma and electromagnetic field data from Cluster C1 and C4 are presented in Figure 7.

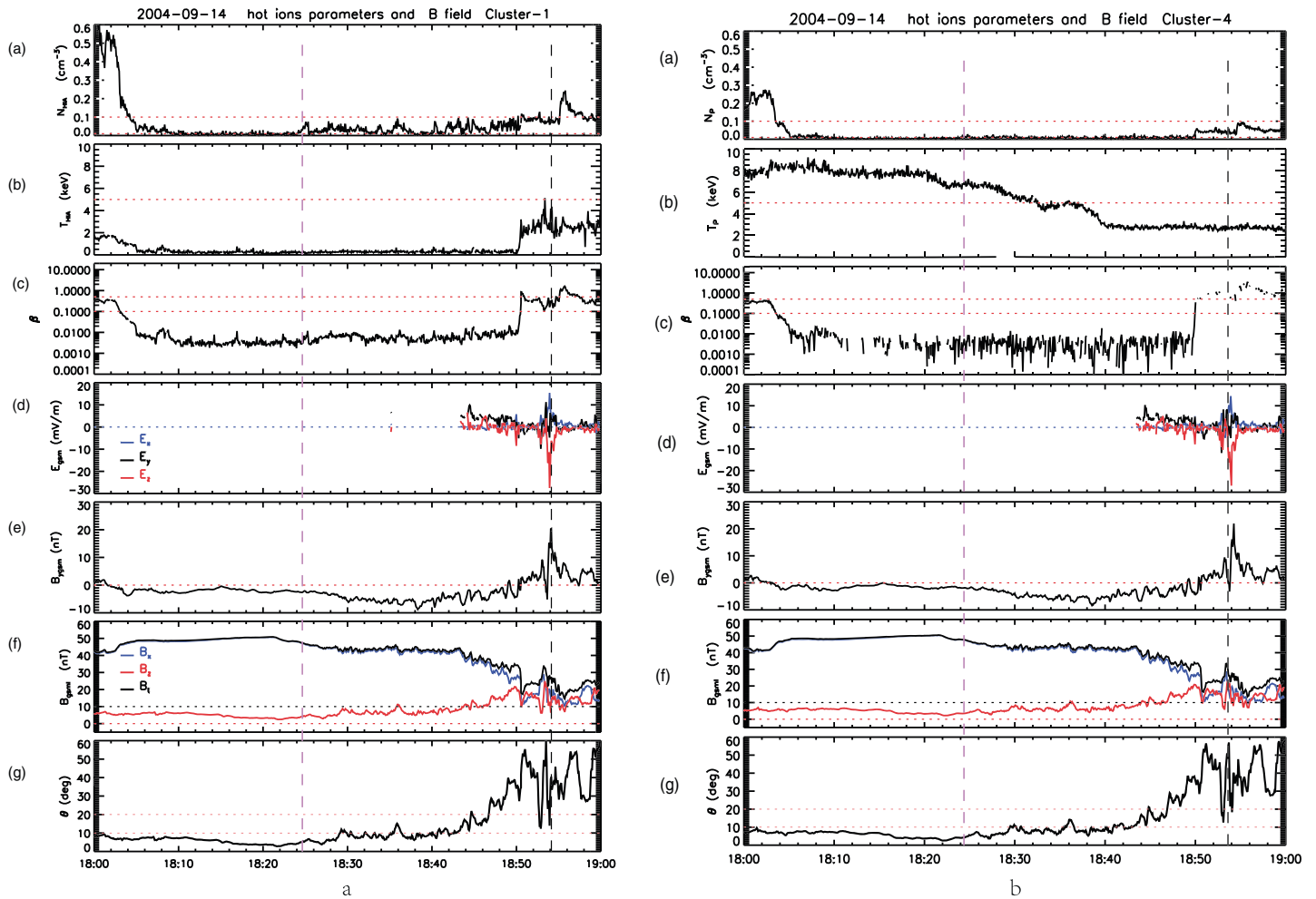


Figure 7. The plasma and electromagnetic field detected by Cluster C1 and C4 in the interval of 18:00 UT to 19:00 UT on 14 September 2004 in the magnetotail. The figure formation is the same as Figure 2.

Figure 7 presents the plasma and electromagnetic field observed by Cluster C1 and C4 during the intense substorm on 14 September 2004. The figure format is the same as Figure 2. The vertical dotted purple line marks the beginning time of substorm expansion phase, ~ 18:24 UT. After this time, the ion number density has a slight increase as shown in Figure 7a and the magnetic field magnitude B_t and the B_x component both decrease, but the B_z component and the magnetic elevation angle both increase slightly. At the second dipolarization, ~18:50 UT, a sharp increase in ion temperature, plasma beta value from 0.01 to 0.5, and the magnetic elevation angle from 25° to 55° were observed by Cluster C1 and C4 during this enhancement of the substorm expansion phase. At this time the B_y component is approaching to zero. Four minutes later, at about 18:54 UT, the significant disturbance of the E_z and B_y components is detected, which is marked by vertical dotted black line Figure 7. During the second dipolarization the maximum value of the fluctuation of the $-E_z$ and B_y is 25 mV/m and 20 nT. Cluster observed significant unipolar fluctuations in the PSBL at ~18:54 UT.

The energy flux of O^+ ions from Cluster C1 during the period of 18:00 UT to 19:00 UT on 14 September 2004 is presented in Figure 8a. The pitch angle distribution of O^+ ions with energy range from 40 eV to 1 keV, 1 keV to 10 keV, and 10 keV to 40 keV is shown in Figures 8b–8d, respectively. The low-energy O^+ ion distribution changed from the quasi-parallel to quasi-perpendicular direction at the first magnetic dipolarization time around 18:24 UT as shown in Figure 8b. In the interval time of 18:50 UT to 18:56 UT, energy flux of O^+ ions with 1–10 keV increased significantly and these O^+ ions were mainly

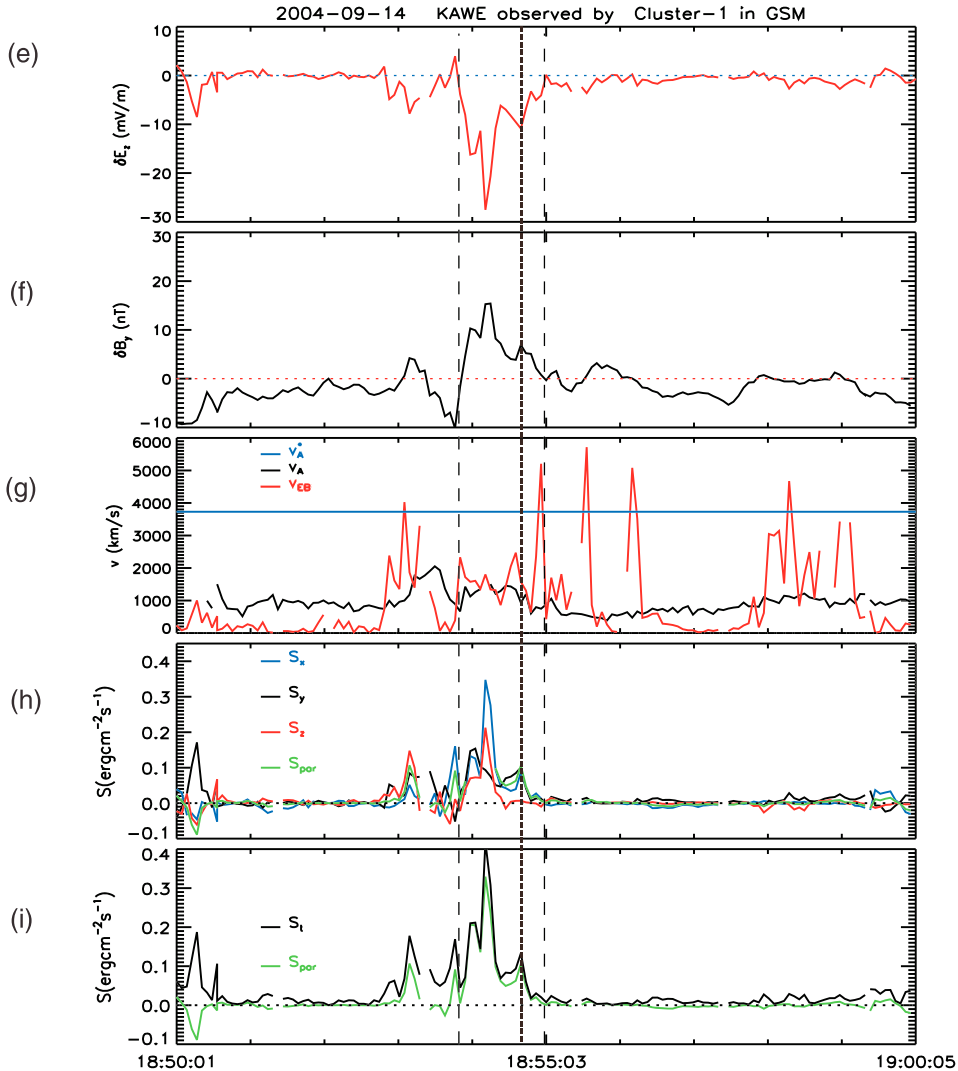
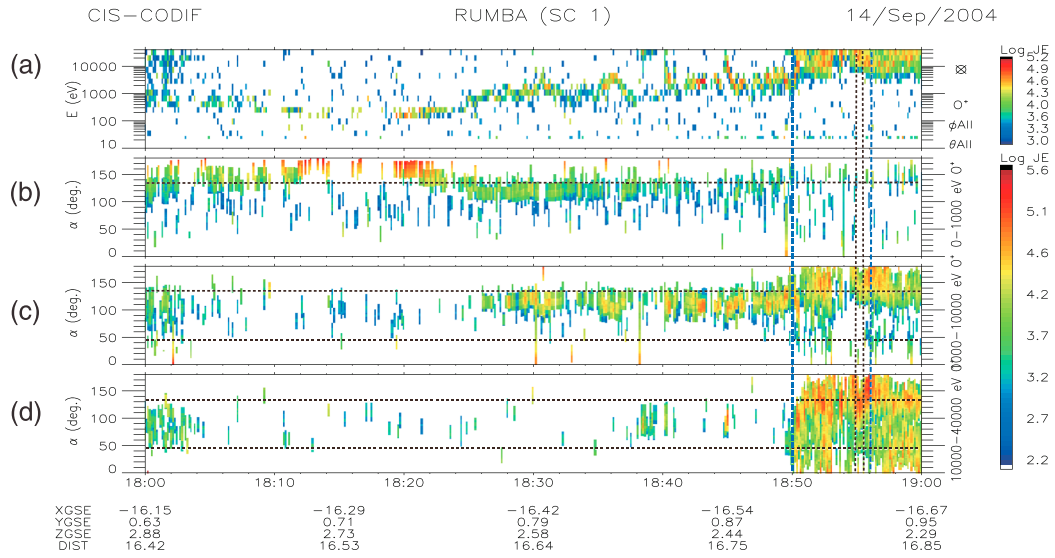


Figure 8. The O^+ ion energy spectrogram flux obtained from CODIF and unipolar electromagnetic field fluctuations observed by Cluster C1 during intense substorm on 14 September 2004. The figure formation is the same as Figure 3.

perpendicular pitch angle distribution, as presented in Figure 8c. As shown in Figures 7c and 7f, the plasma beta is less than 0.5 and the x component of the magnetic field is around 30 nT, approaching the total magnetic field value. These two parameters indicate that SC located at the PSBL during the period of 18:50 UT to 18:56 UT. Within this time interval the intensive unipolar electromagnetic fluctuation with negative E_z and positive B_y is observed, which are presented in Figures 8e and 8f, respectively.

Figure 8e presents that the magnitude of electric field pluses δE_z is -25 mV/m. The corresponding δB_y fluctuations are ~ 12 nT, as shown in Figure 8f. Figure 8g shows that the observed ratio $\delta E_z/\delta B_y$ for intense pulses is from 1,000 km/s to 5,800 km/s. This ratio $\delta E_z/\delta B_y$ is larger than v_A during this intense negative E_z intervals. The Poynting flux, as shown in Figures 8h and 8i, is mostly along the magnetic field direction toward Earth, 0.2 erg $\text{cm}^{-2} \text{s}^{-1}$. The $\delta E_z/\delta B_y$ ratio and unipolar electromagnetic pulses also provide strong evidences that these intense unipolar perturbations are KAWE (Duan et al., 2016).

During this intense substorm dipolarization, the similar observation results from Cluster C4 are presented in Figure 9. Because of the distance from Cluster C4 to the plasma sheet is smaller than the distance from Cluster C1, Cluster C4 first detected the PSBL at around 18:50 UT.

The unipolar pulse electric field of KAWE was both observed by C1 and C4 in the period of 18:53:50 UT to 18:55:00 UT in the PSBL, as shown in Figures 8e and 9e. During this period energetic O^+ ions were accelerated in the direction perpendicular to the background magnetic field, as shown in Figures 8c and 8d, and 9c and 9d, Figures 10a and 10b show two examples of 2-D cuts (the v_x - v_y plane and v_x - v_z plane) through the 3-D distributions of O^+ ion velocity observed by C4 at 18:54:43 UT and 18:54:51 UT, which are marked by the vertical dotted lines in Figure 9. Similarly, Figures 10c and 10d present the O^+ ion velocity distributions by C1 at 18:54:44 UT and 18:54:53 UT, which are marked by the vertical dotted lines in Figure 8. These cuts display that energetic O^+ ions (>1 keV) mainly flow in the southward direction with negative value of the v_z component. It is coincident of the pitch angle distribution of O^+ ions in the direction perpendicular to the magnetic field, as marked by the vertical dotted lines in Figures 8 and 9. The increase in magnitude of $-v_z$ is from 400 km/s to 700 km/s. Then O^+ ions can be transferred from PSBL into the plasma sheet.

The intense unipolar electromagnetic pulses observed by Cluster C1 and C4 are identified as KAWE, as shown in Figures 8e–8g and 9e–9g. During the intense KAWE period, O^+ ions were accelerated in the direction perpendicular to the background magnetic field, as shown with perpendicular pitch angle distribution of energetic O^+ ions (>1 keV) in Figures 8c and 9c, and the magnitude of southward V_z component of O^+ ion enhancement in Figure 10. As a result, O^+ ions can pass through the PSBL into the central plasma sheet.

2.4. Discussions on the Acceleration Mechanism for O^+ Ions at PSBL

In the above section, we have shown O^+ ions accelerated by KAWE at the PSBL in the magnetotail during two intense substorms dipolarizations. The intense unipolar electric field fluctuation toward southward, that is, $E_z \sim -20$ mV/m and magnetic field fluctuations toward duskside are detected by Cluster C1 and C4, as shown in Figures 3e and 3f, 4e and 4f, 8e and 8f, and 9e and 9f. This intense unipolar pulse electric field of KAWE existing in the PSBL with thickness $\sim 1,000$ km is enough for O^+ ions energized from 1 keV to several tens keV in the direction perpendicular to the magnetic field, as presented in Figures 3, 4, 8, and 9. Corresponding to the intense southward electric field of KAWE mode, the velocity V_z component of O^+ ions is very high and in the southward direction as shown in Figures 5 and 10. During 31 August 2004 substorm, the value of the Z component electric field was about $E_z \sim -12$ mV/m at $\sim 10:23$ UT in the PSBL as shown in Figure 3e. For O^+ passing through the PSBL, this field can provide energy of $\sim 10^{-15}$ J. At this time we can find that O^+ ion velocity significantly enhanced from $-V_z \sim 400$ km/s to $-V_z \sim 600$ km/s as shown in Figures 5c and 5d. The energy of O^+ ion increases with $\sim 10^{-15}$ J. Similarly, during 14 September 2004 substorm, the value of the Z component electric field was about $E_z \sim -10$ mV/m at $\sim 18:54$ UT as shown in Figure 9e. We can also find that O^+ ion velocity significantly enhanced from $V_z \sim -500$ km/s to $V_z \sim -600$ km/s as shown in Figures 10c and 10d. The quantity relationship between the wave electric energy and O^+ ion increasing kinetic energy provides confident evidence that KAWE can efficiently accelerate O^+ ions in the PSBL during intense substorm dipolarizations.

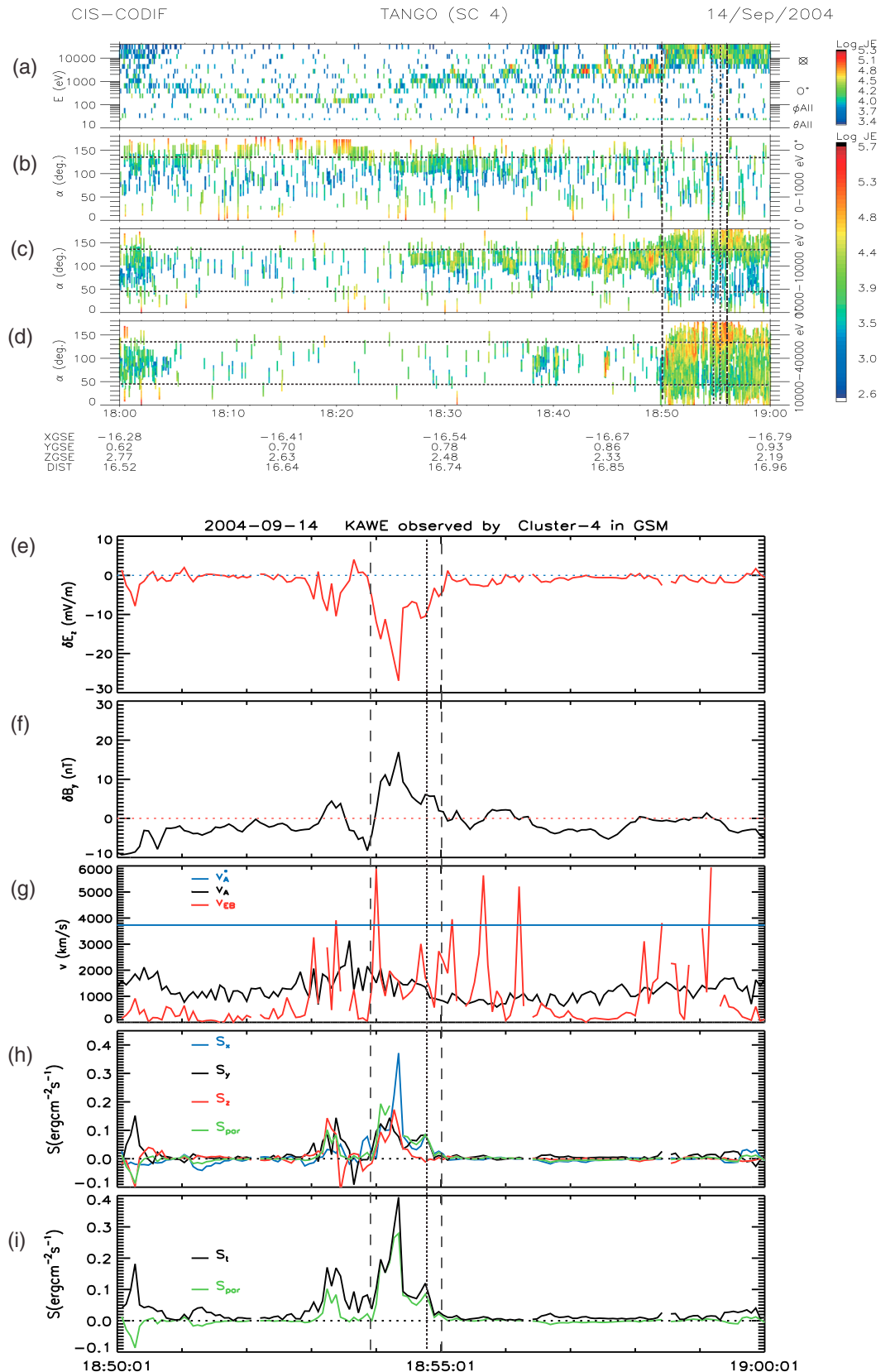


Figure 9. The O^+ ion energy spectrogram flux obtained from CODIF and unipolar electromagnetic field fluctuations observed by Cluster C4 during intense substorm on 14 September 2004. The figure formation is the same as Figure 4.

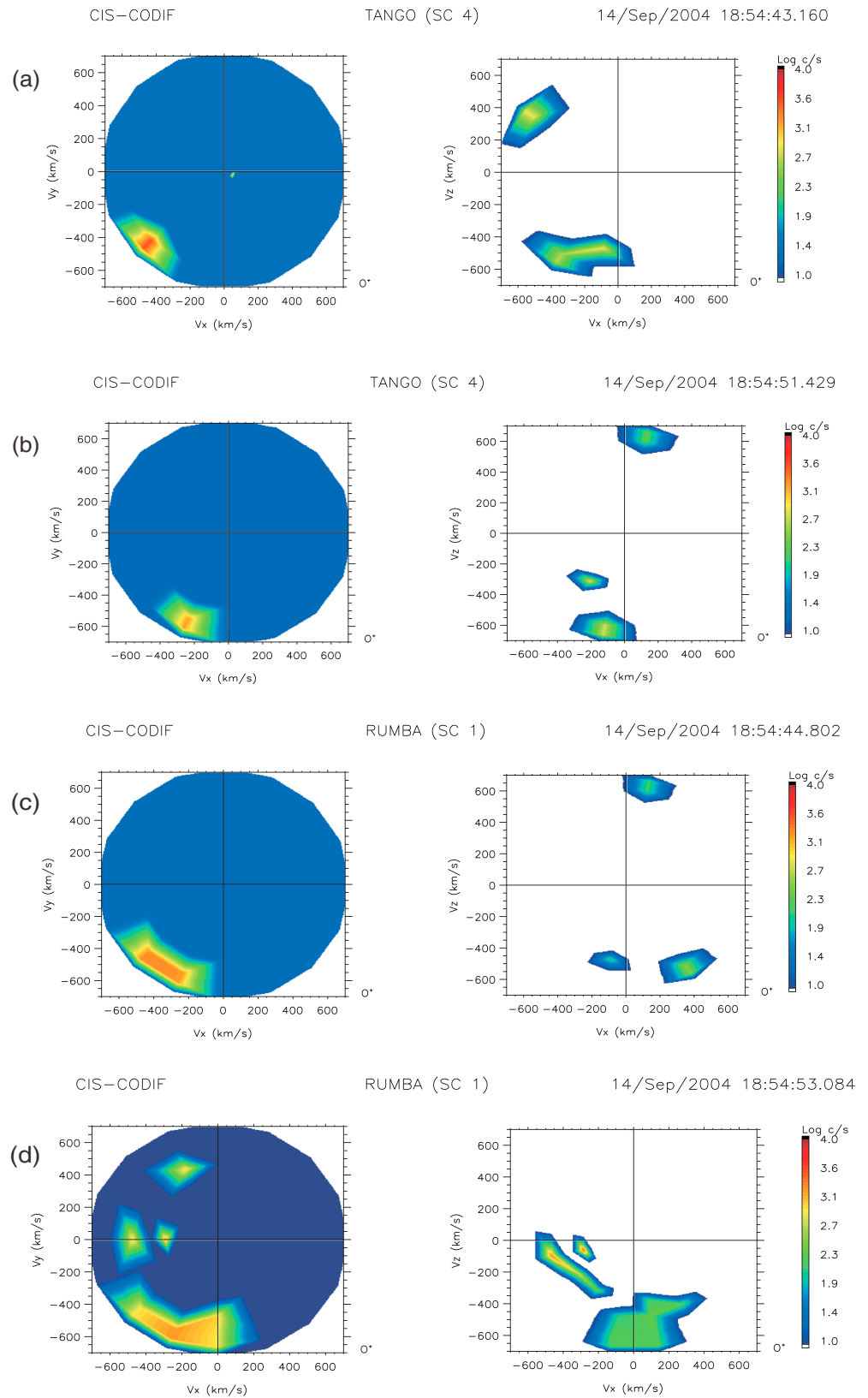


Figure 10. Two-dimensional cuts of the three-dimensional O^+ ion velocity distributions obtained by CODIF/C1 at 18:54:44 UT and 18:54:53 UT, respectively, and by CODIF/C4 at 18:54:43 UT and 18:54:51 UT, respectively, as marked by the vertical dotted line in Figures 8 and 9, respectively.

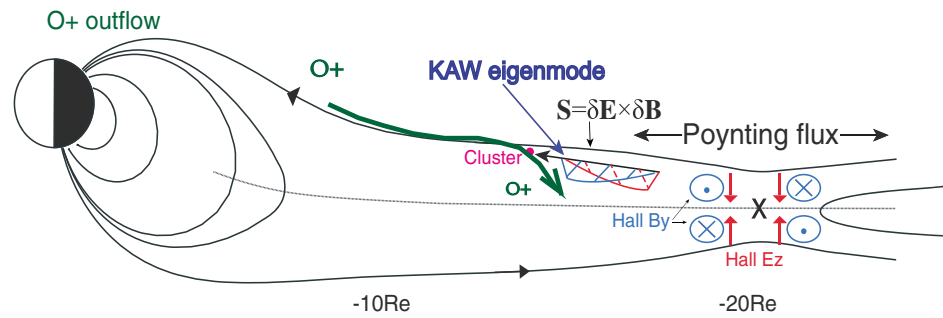


Figure 11. A cartoon illustrates the O^+ ion transfer and acceleration during substorm dipolarization in the NEPS.

On the other hand, the gyroradius of O^+ ions with energy ~ 10 keV is comparable to the spatial scale of the PSBL, that is, $\sim 1,000$ km. Thus, O^+ ions can be energized by KAWs with the large perpendicular electric field, $E_z \sim -20$ mV/m, at the PSBL in the magnetotail during intense substorm dipolarization as mentioned above. This acceleration is very useful for O^+ ions from the lobe passed through the PSBL into the center plasma sheet in the magnetotail. Figure 11 provides a clear pathway of O^+ ions accelerated by KAWs in the PSBL from the lobe into the plasma sheet.

Several previous researches reported that ions perpendicular acceleration was caused by the $E \times B$ drift velocity increase in the PSBL (e.g., Grigorenko, Burinskaya, et al., 2010; Grigorenko, Koleva, et al., 2010; Grigorenko et al., 2011; Hirahara et al., 1994; Takada, Seki, Hirahara, Fujimoto, et al., 2005; Takada, Seki, Hirahara, Terasawa, et al., 2005). This drift is the reason that ions transported from the lobe to the plasma sheet. The strong E_y and B_x components are useful under this circumstance. But in our investigation, the electric field is dominantly in the north-to-south direction (E_z). Then the $E \times B$ drift cannot illustrate O^+ ions transferring from the lobe to the central plasma sheet. Lindstedt et al. (2010) reported that O^+ ions can be accelerated by the strong perpendicular electric field in localized size to several keV in the boundary between the high-latitude cusp and the lobe. They pointed out that this intense electric field was related to a reconnection separatrix region. This intense perpendicular electric field is similar to the strong electric field of KAWs.

As mentioned by Ono et al. (2009) and Fok et al. (2006), O^+ ions can be accelerated during substorm dipolarization because O^+ ions have a gyroperiod in the NEPS comparable with the dipolarization period, that is, a few minutes. But the induced electric field in substorm onset location is only intense at the inner edge of plasma sheet, that is, in the vicinity of substorm onset location. For our observation, Cluster is located at $X \sim -16 R_E$ in the midtail PSBL. O^+ ions accelerated during substorm dipolarization is not by this intense induced electric field near substorm onset location. It is by the strong unipolar electric field accompanied by the KAWs in the PSBL (Duan et al., 2016). This result can be clearly evidenced by our two events presented above.

The substorms are of maximum value of AE index around $\sim 1,000$ nT and AU index larger than ~ 200 nT in the later growth phase. Daglis et al. (1994) reported that energization of O^+ ions in the near-Earth magnetotail had a close correlation with the magnitude of AU index in the later growth phase. During the expansion phase of these two intense substorms the energy flux of O^+ ions increased, and the pitch angle distribution of energetic O^+ ions changed significantly when AE index larger than 500 nT, such as after 10:20 UT on 31 August 2004 and after 18:30 UT on 14 September 2004 in Figures 3 and 8, respectively. Our observation results in the magnetotail are consistent with that of Daglis et al. (1994).

3. Summary

Using Cluster measurements, we provide evidence that O^+ ions are energized by KAWs in the plasma sheet boundary layer during intense substorm (with AE index larger than 500 nT) dipolarization. The thickness of the PSBL during intense substorm is comparable for the gyroradius of energized O^+ ions with tens of keV. These O^+ ions encountered unipolar electric field of the KAWs and are energized efficiently. The results of our observations can be summarized as the following.

The energy flux of O^+ ions with energy larger than 1 keV increases significantly during the dipolarization of intense substorms, with the AE index usually larger than 500 nT, in the magnetotail plasma sheet. At the beginning time of the first substorm dipolarization, the pitch angle distribution of these energetic oxygen ions changes from the quasi-parallel direction to the quasi-perpendicular direction to the background magnetic field.

O^+ ions are energized by the KAWE mostly in the perpendicular direction to the background magnetic field during the expansion phase of intense substorms. As a result of magnetic reconnection in the magnetotail $X \sim -20 R_E$, the KAWE with unipolar electric field directing to the center plasma sheet exists in the plasma sheet boundary layer in the magnetotail (Dai, 2009; Dai et al., 2011; Duan et al., 2016). The intense unipolar electric field, $E_z \sim -20$ mV/m, can efficiently accelerate O^+ ions in the direction perpendicular to the magnetic field.

KAWE can play an important role in O^+ ion transfer process from the lobe and plasma sheet boundary layer into the central plasma sheet during intense substorms. O^+ ion origin from the cusp or auroral region can be accelerated by the KAWE in the plasma sheet boundary layer and then directly enter into the central plasma sheet with energy of tens of keV. This intense wave electric power can efficiently energize O^+ ions with energy of tens of keV.

Acknowledgments

We acknowledge the use of data from the ESA Cluster Science Archive (<http://www.cosmos.esa.int/web/csa>). We thank the FGM, CIS, and EFW instrument teams. The AE index was provided by Data Analysis Center for Geomagnetism and Space Magnetism in Kyoto, Japan. This work is supported by the National Natural Science Foundation of China grants 41674167, 41574161, and 41231067 and the Specialized Research Fund for State Key Laboratories.

References

- Baker, D. N., Fritz, T. A., Birn, J., Lennartsson, W., Wilken, B., & Kroehl, H. W. (1985). The role of heavy ionospheric ions in the localization of substorm disturbances on March 22, 1979: CDAW 6. *Journal of Geophysical Research*, *90*(A2), 1273–1281. <https://doi.org/10.1029/JA090iA02p01273>
- Baker, D. N., Hones, E. W. Jr., Young, D. T., & Birn, J. (1982). The possible role of ionospheric oxygen in the initiation and development of plasma sheet instabilities. *Geophysical Research Letters*, *9*(12), 1337–1340. <https://doi.org/10.1029/GL009i012p01337>
- Balogh, A., Carr, C. M., Acuña, M. H., Dunlop, M. W., Beek, T. J., Brown, P., ... Schwingenschuh, K. (2001). The Cluster magnetic field investigation: Overview of in-flight performance and initial results. *Annales de Geophysique*, *19*(10/12), 1207–1217. <https://doi.org/10.5194/angeo-19-1207-2001>
- Baumjohann, W., Hesse, M., Kokubun, S., Mukai, T., Nagai, T., & Petrukovich, A. A. (1999). Substorm dipolarization and recovery. *Journal of Geophysical Research*, *104*(A11), 24,995–25,000. <https://doi.org/10.1029/1999JA900282>
- Chen, L., Wu, D. J., & Huang, J. (2013). Kinetic Alfvén wave instability driven by field-aligned currents in a low-beta plasma. *Journal of Geophysical Research: Space Physics*, *118*, 2951–2957. <https://doi.org/10.1002/jgra.50332>
- Chen, L., Wu, D. J., Zhao, G. Q., Tang, J. F., & Huang, J. (2015). A possible mechanism for the formation of filamentous structures in magnetoplasmas by kinetic Alfvén waves. *Journal of Geophysical Research: Space Physics*, *120*, 61–69. <https://doi.org/10.1002/2014JA020742>
- Daglis, I. A., & Axford, W. I. (1996). Fast ionospheric response to enhanced activity in geospace: Ion feeding of the inner magnetotail. *Journal of Geophysical Research*, *101*(A3), 5047–5065. <https://doi.org/10.1029/95JA02592>
- Daglis, I. A., Livi, S., Sarris, E. T., & Wilken, B. (1994). Energy density of ionospheric and solar wind origin ions in the near-Earth magnetotail during substorms. *Journal of Geophysical Research*, *99*(A4), 5691–5703. <https://doi.org/10.1029/93JA02772>
- Dai, L. (2009). Collisionless magnetic reconnection via Alfvén eigenmodes. *Physical Review Letters*, *102*(24), 245003. <https://doi.org/10.1103/PhysRevLett.102.245003>
- Dai, L., Takahashi, K., Wygant, J. R., Chen, L., Bonnell, J., Cattell, C. A., ... Spence, H. E. (2013). Excitation of poloidal standing Alfvén waves through drift resonance wave-particle interaction. *Geophysical Research Letters*, *40*, 4127–4132. <https://doi.org/10.1002/grl.50800>
- Dai, L., Wang, C., Angelopoulos, V., & Glassmeier, K.-H. (2015). In situ evidence of breaking the ion frozen-in condition via the non-gyrotropic pressure effect in magnetic reconnection. *Annales de Geophysique*, *33*(9), 1147–1153. <https://doi.org/10.5194/angeo-33-1147-2015>
- Dai, L., Wang, C., Duan, S., He, Z., Wygant, J. R., Cattell, C. A., ... Tang, X. (2015). Near-Earth injection of MeV electrons associated with intense dipolarization electric fields: Van Allen Probes observations. *Geophysical Research Letters*, *42*, 6170–6179. <https://doi.org/10.1002/2015GL064955>
- Dai, L., Wang, C., Zhang, Y., Lavraud, B., Burch, J., Pollock, C., & Torbert, R. B. (2017). Kinetic Alfvén wave explanation of the Hall fields in magnetic reconnection. *Geophysical Research Letters*, *44*, 634–640. <https://doi.org/10.1002/2016GL071044>
- Dai, L., Wygant, J. R., Cattell, C., Dombeck, J., Thaller, S., Mouikis, C., ... Rème, H. (2011). Cluster observations of surface waves in the ion jets from magnetotail reconnection. *Journal of Geophysical Research*, *116*, A12227. <https://doi.org/10.1029/2011JA017004>
- Dai, L., Wygant, J. R., Cattell, C. A., Thaller, S., Kersten, K., Breneman, A., ... Tao, X. (2014). Evidence for injection of relativistic electrons into the Earth's outer radiation belt via intense substorm electric fields. *Geophysical Research Letters*, *41*, 1133–1141. <https://doi.org/10.1002/2014GL059228>
- Delcourt, D. C., Sauvaud, J. A., & Pedersen, A. (1990). Dynamics of simple-particle orbits during substorm expansion phase. *Journal of Geophysical Research*, *95*(A12), 20853–20,865. <https://doi.org/10.1029/JA095iA12p20853>
- Duan, S., Dai, L., Wang, C., Lui, A. T. Y., Liu, Z., He, Z., ... Rème, H. (2015). Cluster observations of unusually high concentration of energetic O^+ carried by flux ropes in the nightside high-latitude magnetosheath during a storm initial phase. *Journal of Geophysical Research: Space Physics*, *120*, 8317–8326. <https://doi.org/10.1002/2015JA021306>
- Duan, S. P., Dai, L., Wang, C., Liang, J., Lui, A. T. Y., Chen, L. J., ... Angelopoulos, V. (2016). Evidence of kinetic Alfvén eigenmode in the near-earth magnetotail during substorm expansion phase. *Journal of Geophysical Research: Space Physics*, *121*, 4316–4330. <https://doi.org/10.1002/2016JA022431>
- Duan, S. P., Liu, Z. X., Liang, J., Zhang, Y. C., & Chen, T. (2011). Multiple magnetic dipolarizations observed by THEMIS during a substorm. *Annales de Geophysique*, *29*(2), 331–339. <https://doi.org/10.5194/angeo-29-331-2011>
- Fok, M., Moore, T. E., Brandt, P. C., Delcourt, D. C., Slinker, S. P., & Fedder, J. A. (2006). Impulsive enhancements of oxygen ions during substorms. *Journal of Geophysical Research*, *111*, A10222. <https://doi.org/10.1029/2006JA011839>

- Frey, H. U., Mende, S. B., Angelopoulos, V., & Donovan, E. F. (2004). Substorm onset observations by IMAGE-FUV. *Journal of Geophysical Research*, 109, A10304. <https://doi.org/10.1029/2004JA010607>
- Grigorenko, E. E., Burinskaya, T. M., Shevelev, M., Sauvaud, J. A., & Zelenyi, L. M. (2010). Large-scale fluctuations of PSBL magnetic flux tubes induced by the field-aligned motion of highly accelerated ions. *Annales Geophysicae*, 28(6), 1273–1288. <https://doi.org/10.5194/angeo-28-1273-2010>
- Grigorenko, E. E., Koleva, R., Zelenyi, L. M., & Sauvaud, J. A. (2010). Accelerated ions observed in the plasma sheet boundary layer: Beams or streams? *Geomagnetism and Aeronomy*, 50(6), 720–732. <https://doi.org/10.1134/S0016793210060034>
- Grigorenko, E. E., Zelenyi, L. M., Dolgonosov, M. S., Artemiev, A. V., Owen, C. J., Sauvaud, J. A., ... Hirai, M. (2011). Non-adiabatic ion acceleration in the Earth magnetotail and its various manifestations in the plasma sheet boundary layer. *Space Science Reviews*, 164(1–4), 133–181. <https://doi.org/10.1007/s11214-011-9858-9>
- Gustafsson, G., André, M., Carozzi, T., Eriksson, A. I., Fälthammar, C.-G., Grard, R., ... Wahlund, J.-E. (2001). First results of electric field and density observations by CLUSTER EFW based on initial months of operation. *Annales de Geophysique*, 19(10/12), 1219–1240. <https://doi.org/10.5194/angeo-19-1219-2001>
- Hirahara, M., Nakamura, M., Terasawa, T., Mukai, T., Saito, Y., Yamamoto, T., ... Kokubun, S. (1994). Acceleration and heating of cold ion beams in the plasma sheet boundary layer observed with GEOTAIL. *Geophysical Research Letters*, 21(25), 3003–3006. <https://doi.org/10.1029/94GL02109>
- Keika, K., Kistler, L. M., & Brandt, P. C. (2013). Energization of O^+ ions in the Earth's inner magnetosphere and the effects on ring current buildup: A review of previous observations and possible mechanisms. *Journal of Geophysical Research: Space Physics*, 118, 4441–4464. <https://doi.org/10.1002/jgra.50371>
- Keiling, A. (2009). Alfvén waves and their roles in the dynamics of the Earth's magnetotail: A review. *Space Science Reviews*, 142(1–4), 73–156. <https://doi.org/10.1007/s11214-008-9463-8>
- Khotyaintsev, Y., Lindqvist, P.-A., Eriksson, A. I., & André, M. (2010). The EFW data in the CAA, the Cluster Active Archive, studying the Earth's space plasma environment. In H. Laakso, M. G. T. Taylor, & C. P. Escoubert (Eds.), *Astrophysics and Space Science Proceedings* (pp. 97–108). Berlin: Springer.
- Kistler, L. M. (2017). The impact of O^+ on magnetotail dynamics, magnetosphere-ionosphere coupling in the solar system. In C. R. Chappell, et al. (Eds.), *Geophysical Monograph* (1st ed., Vol. 222, pp. 79–89). Hoboken, NJ: American Geophysical Union, John Wiley.
- Kistler, L. M., Moebius, E., Klecker, B., Gloeckler, G., Ipavich, F. M., & Hamilton, D. C. (1990). Spatial variations in the suprathermal ion distributions during substorms in the plasma sheet. *Journal of Geophysical Research*, 95(A11), 18871–18,885. <https://doi.org/10.1029/JA095iA11p18871>
- Klimushkin, D. Y., & Mager, P. N. (2014). The Alfvén wave parallel electric field in non-uniform space plasma. *Astrophysics and Space Science*, 350(2), 579–583. <https://doi.org/10.1007/s10509-013-1774-x>
- Kronberg, E. A., Ashour-Abdalla, M., Dandouras, I., Delcourt, D. C., Grigorenko, E. E., Kistler, L. M., ... Zelenyi, L. M. (2014). Circulation of heavy ions and their dynamical effects in the magnetosphere: Recent observations and models. *Space Science Reviews*, 184(1–4), 173–235. <https://doi.org/10.1007/s11214-014-0104-0>
- Laakso, H., Taylor, M. G. T., & Escoubert, C. P. (2010). The Cluster Active Archive, Studying the Earth's Space Plasma Environment. In *Astrophysics and Space Science Proceedings* (Ed.). Berlin: Springer. <https://doi.org/10.1007/978-90-481-3499-1>
- Lee, L. C., Johnson, J. R., & Ma, Z. W. (1994). Kinetic Alfvén waves as a source of plasma transport at the dayside magnetopause. *Journal of Geophysical Research*, 104, 17,405–17,411.
- Lennartsson, W., & Shelley, E. G. (1986). Survey of 0.1- to 16-keV/e plasma sheet ion composition. *Journal of Geophysical Research*, 91(A3), 3061–3076. <https://doi.org/10.1029/JA091iA03p03061>
- Liang, J., Lin, Y., Johnson, J. R., Wang, X., & Wang, Z.-X. (2016). Kinetic Alfvén waves in three-dimensional magnetic reconnection. *Journal of Geophysical Research: Space Physics*, 121, 6526–6548. <https://doi.org/10.1002/2016JA022505>
- Liao, J., Kistler, L. M., Mouikis, C. G., Klecker, B., & Dandouras, I. (2015). Acceleration of O^+ from the cusp to the plasma sheets. *Journal of Geophysical Research: Space Physics*, 120, 1022–1034. <https://doi.org/10.1002/2014JA020341>
- Liao, J., Kistler, L. M., Mouikis, C. G., Klecker, B., Dandouras, I., & Zhang, J. C. (2010). Statistical study of O^+ transport from the cusp to the lobes with Cluster CODIF data. *Journal of Geophysical Research*, 115, A00J15. <https://doi.org/10.1029/2010JA015613>
- Lin, Y., Johnson, J. R., & Wang, X. (2012). Three-dimensional mode conversion associated with kinetic Alfvén waves. *Physical Review Letters*, 109(12), 125003. <https://doi.org/10.1103/PhysRevLett.109.125003>
- Lindstedt, T., Khotyaintsev, Y. V., Vaivads, A., André, M., Nilsson, H., & Waara, M. (2010). Oxygen energization by localized perpendicular electric fields at the cusp boundary. *Geophysical Research Letters*, 37, L09103. <https://doi.org/10.1029/2010GL043117>
- Lui, A. T. Y., Liou, K., Nosé, M., Ohtani, S., Williams, D. J., Mukai, T., ... Kokubun, S. (1999). Near-Earth dipolarization: Evidence for a non-MHD process. *Geophysical Research Letters*, 26(19), 2905–2908. <https://doi.org/10.1029/1999GL003620>
- Maggiolo, R., & Kistler, L. M. (2014). Spatial variation in the plasma sheet composition: Dependence on geomagnetic and solar activity. *Journal of Geophysical Research: Space Physics*, 119, 2836–2857. <https://doi.org/10.1002/2013JA019517>
- Mouikis, C. G., Kistler, L. M., Liu, Y. H., Klecker, B., Korth, A., & Dandouras, I. (2010). H^+ and O^+ content of the plasma sheet at 15–19 Re as a function of geomagnetic and solar activity. *Journal of Geophysical Research*, 115, A00J16. <https://doi.org/10.1029/2010JA015978>
- Nagai, T. (1982). Observed magnetic substorm signatures at synchronous altitude. *Journal of Geophysical Research*, 87(A6), 4405–4417. <https://doi.org/10.1029/JA087iA06p04405>
- Nakamura, R., Retinò, A., Baumjohann, W., Volwerk, M., Erkaev, N., Klecker, B., ... Khotyaintsev, Y. (2009). Evolution of dipolarization in the near-Earth current sheet induced by earthward rapid flux transport. *Annales de Geophysique*, 27(4), 1743–1754. <https://doi.org/10.5194/angeo-27-1743-2009>
- Nilsson, H., Hamrin, M., Pitkanen, T., Karlsson, T., Slapak, R., Andersson, L., ... Vaivads, A. (2016). Oxygen ion response to proton bursty bulk flows. *Journal of Geophysical Research: Space Physics*, 121, 7535–7546. <https://doi.org/10.1002/2016JA022498>
- Nosé, M., Lui, A. T. Y., Ohtani, S., Mauk, B. H., McEntire, R. W., Williams, D. J., ... Yumoto, K. (2000). Acceleration of oxygen ions of ionospheric origin in the near-Earth magnetotail during substorms. *Journal of Geophysical Research*, 105(A4), 7669–7677. <https://doi.org/10.1029/1999JA000318>
- Ohtani, S., Nosé, M., Christon, S. P., & Lui, A. T. Y. (2011). Energetic O^+ and H^+ ions in the plasma sheet: Implications for the transport of ionospheric ions. *Journal of Geophysical Research*, 116, A10211. <https://doi.org/10.1029/2011JA016532>
- Ono, Y., Nose, M., Christon, S. P., & Lui, A. T. Y. (2009). The role of magnetic field fluctuations in nonadiabatic acceleration of ions during dipolarization. *Journal of Geophysical Research*, 114, A05209. <https://doi.org/10.1029/2008JA013918>
- Peromian, V., El-Alaoui, M., Abdalla, M. A., & Zelenyi, L. M. (2006). Dynamics of ionospheric O^+ ions in the magnetosphere during the 24–25 September 1998 magnetic storm. *Journal of Geophysical Research*, 111, A12203. <https://doi.org/10.1029/2006JA011790>

- Rème, H., Aoustin, C., Bosqued, J. M., Dandouras, I., Lavraud, B., Sauvaud, J. A., ... Sonnerup, B. (2001). First multispacecraft ion measurements in and near the Earth's magnetosphere with the identical Cluster ion spectrometry (CIS) experiment. *Annales de Geophysique*, *19*(10/12), 1303–1354. <https://doi.org/10.5194/angeo-19-1303-2001>
- Sauvaud, J. A., Jacquey, C., Oka, M., Palin, L., Fruit, G., Kistler, L. M., ... Grigorenko, E. (2012). A study of the changes of the near-Earth plasma sheet and lobe driven by multiple substorms: Comparison with a full particle simulation of reconnection. *Journal of Geophysical Research*, *117*, A01221. <https://doi.org/10.1029/2011JA017033>
- Seki, K., Elphic, R. C., Hirahara, M., Terasawa, T., & Mukai, T. (2001). On atmospheric loss of oxygen ions from Earth through magnetospheric processes. *Science*, *291*(5510), 1939–1941. <https://doi.org/10.1126/science.1058913>
- Takada, T., Seki, K., Hirahara, M., Fujimoto, M., Saito, Y., Hayakawa, H., & Mukai, T. (2005). Statistical properties of low-frequency waves and ion beams in the plasma sheet boundary layer: Geotail observations. *Journal of Geophysical Research*, *110*, A02204. <https://doi.org/10.1029/2004JA010395>
- Takada, T., Seki, K., Hirahara, M., Terasawa, T., Hoshino, M., & Mukai, T. (2005). Two types of PSBL ion beam observed by Geotail: Their relation to low frequency electromagnetic waves and cold ion energization. *Advances in Space Research*, *36*(10), 1883–1889. <https://doi.org/10.1016/j.asr.2003.09.075>
- Welling, D. T., André, M., Dandouras, I., Delcourt, D., Fazakerley, A., Fontaine, D., ... Yau, A. (2015). The Earth: Plasma sources, losses, and transport processes. *Space Science Reviews*, *192*(1-4), 145–208. <https://doi.org/10.1007/s11214-015-0187-2>
- Winglee, R. M., & Harnett, E. (2011). Influence of heavy ionospheric ions on substorm onset. *Journal of Geophysical Research*, *116*, A11212. <https://doi.org/10.1029/2011JA016447>
- Wu, D. J., & Chen, L. (2013). Excitation of kinetic Alfvén waves by density striation in magneto-plasmas. *The Astrophysical Journal*, *771*(1), 3. <https://doi.org/10.1088/0004-637X/771/1/3>
- Wygant, J. R., Cattell, C. A., Lysak, R., Song, Y., Dombek, J., McFadden, J., ... Mouikis, C. (2005). Cluster observations of an intense normal component of the electric field at a thin reconnecting current sheet in the tail and its role in the shock-like acceleration of the ion fluid into the separatrix region. *Journal of Geophysical Research*, *110*, A09206. <https://doi.org/10.1029/2004JA010708>
- Yau, A. W., & André, M. (1997). Sources of ion outflow in the high latitude ionosphere. *Space Science Reviews*, *80*(1/2), 1–25. <https://doi.org/10.1023/A:1004947203046>
- Yau, A. W., Howarth, A., Peterson, W. K., & Abe, T. (2012). Transport of thermal-energy ionospheric oxygen (O^+) ions between the ionosphere and the plasma sheet and ring current at quiet times preceding magnetic storms. *Journal of Geophysical Research*, *117*, A07215. <https://doi.org/10.1029/2012JA017803>
- Yau, A. W., Shelley, E. G., Peterson, W. K., & Lenchyshyn, L. (1985). Energetic auroral and polar ion outflow at DE 1 altitudes: Magnitude, composition, magnetic activity dependence, and long-term variations. *Journal of Geophysical Research*, *90*(A9), 8417–8432. <https://doi.org/10.1029/JA090iA09p08417>
- Yu, Y., & Ridley, A. J. (2013). Exploring the influence of ionospheric O^+ outflow on magnetospheric dynamics: Dependence on the source location. *Journal of Geophysical Research: Space Physics*, *118*, 1711–1722. <https://doi.org/10.1029/2012JA018411>